

Pacific Northwest National Laboratory

Operated by Battelle for the
U.S. Department of Energy

Spent Fuel Dissolution Rates as a Function of Burnup and Water Chemistry

W. J. Gray

June 1998

Prepared for the U.S. Department of Energy
under Contract DE-AC06-76RLO 1830

PNNL-11895

Legacy-700

DISCLAIMER

This report was prepared as an account of work sponsored by an agency of the United States Government. Neither the United States Government nor any agency thereof, nor Battelle Memorial Institute, nor any of their employees, makes any warranty, express or implied, or assumes any legal liability or responsibility for the accuracy, completeness, or usefulness of any information, apparatus, product, or process disclosed, or represents that its use would not infringe privately owned rights. Reference herein to any specific commercial product, process, or service by trade name, trademark, manufacturer, or otherwise does not necessarily constitute or imply its endorsement, recommendation, or favoring by the United States Government or any agency thereof, or Battelle Memorial Institute. The views and opinions of authors expressed herein do not necessarily state or reflect those of the United States Government or any agency thereof.

PACIFIC NORTHWEST NATIONAL LABORATORY

operated by

BATTELLE

for the

UNITED STATES DEPARTMENT OF ENERGY

under Contract DE-AC06-76RLO 1830

Printed in the United States of America

Available to DOE and DOE contractors from the
Office of Scientific and Technical Information, P.O. Box 62, Oak Ridge, TN 37831;
prices available from (615) 576-8401.

Available to the public from the National Technical Information Service,
U.S. Department of Commerce, 5285 Port Royal Rd., Springfield, VA 22161



This document was printed on recycled paper.

Spent Fuel Dissolution Rates as a Function of Burnup and Water Chemistry

W. J. Gray

June 1998

**Prepared for
the U.S. Department of Energy
under Contract DE-AC06-76RLO 1830**

**Pacific Northwest National Laboratory
Richland, Washington 99352**

Summary and Conclusions

To help provide a source term for performance-assessment calculations, dissolution studies on light-water-reactor (LWR) spent fuel have been conducted over the past few years at Pacific Northwest National Laboratory in support of the Yucca Mountain Site Characterization Project. This report describes that work for fiscal years 1996 through mid-1998 and includes summaries of some results from previous years for completeness. The following conclusions were based on the results of various flowthrough dissolution rate tests and on tests designed to measure the inventories of ^{129}I located within the fuel/cladding gap region of different spent fuels:

- 1) Spent fuels with burnups in the range 30 to 50 MWd/kgM all dissolved at about the same rate over the conditions tested. To help determine whether the lack of burnup dependence extends to higher and lower values, tests are in progress or planned for spent fuels with burnups of 13 and ~65 MWd/kgM.
- 2) Oxidation of spent fuel up to the U_4O_{9+x} stage does not have a large effect on intrinsic dissolution rates. However, this degree of oxidation could increase the dissolution rates of relatively intact fuel by opening the grain boundaries, thereby increasing the effective surface area that is available for contact by water. From a disposal viewpoint, this is a potentially more important consideration than the effect on intrinsic rates.
- 3) The gap inventories of ^{129}I were found to be smaller than the fission gas release (FGR) for the same fuel rod with the exception of the rod with the highest FGR. Several additional fuels would have to be tested to determine whether a generalized relationship exists between FGR and ^{129}I gap inventory for U.S. LWR fuels.

Contents

Summary and Conclusions	iii
1.0 Introduction	1
2.0 Experimental Description	3
3.0 Results and Discussion	5
3.1 UO ₂ Matrix Dissolution Rate Tests as a Function of Burnup and Test Condition	7
3.2 Fission Product Dissolution Rates	7
3.3 Dissolution Rate Tests with Oxidized Fuels	8
3.4 ¹²⁹ I Gap Inventories	11
3.5 Tc Dissolution Rates	12
4.0 References	13
Tables 1-4	14-16
Figures 1-12	17-28

1.0 Introduction

This report describes work on the dissolution behavior of spent fuel that was performed at the Pacific Northwest National Laboratory^(a) for the Waste Package Task of the Yucca Mountain Site Characterization Project, which is part of the U.S. Department of Energy's Office of Civilian Radioactive Waste Management. This was done to help provide a source term for use in performance assessment calculations. Progress and results are reported for FY 1996, 1997, and the first half of 1998. In addition, the results of some work performed in previous years has been included for completeness.

Most of the work reported here consisted of flowthrough tests to investigate the dissolution kinetics of different spent fuels over a range of temperatures and water-chemistry conditions. In one test series, spent fuels with different burnups and fission gas releases were tested at two different carbonate/bicarbonate concentrations and two temperatures (total of four test conditions). In a second test series, spent-fuel specimens oxidized to U_4O_{9+x} were tested for comparison with results from tests on unoxidized fuel (UO_2) under the same test conditions.

In addition to the flowthrough tests, results from measurements of the ^{129}I inventories located in the gap regions of several spent fuels are reported.

Because of the short length of this report, all 4 tables and 12 figures were placed at the end.

This work was governed by the following planning and requirements documents:

- (1) Pacific Northwest National Laboratory Quality Assurance Plan, WTC-018, Latest Revision.
- (2) Activity Plan D-20-53b, Flow-Through Dissolution Tests on UO_2 .

Supporting data is documented in Laboratory Record Books BNW 54904 and BNW 55455.

(a) Pacific Northwest National Laboratory is operated by Battelle for the U.S. Department of Energy under Contract DE-AC06-76RLO 1830.

2.0 Experimental Description

Gray and Wilson (1995) described the flowthrough apparatus and test method. Most of the test specimens used in the flowthrough tests consisted of grain-size powder (7 to 28 μm in size, see Table 1). To prepare these specimens, the fuel was removed from its cladding and crushed, followed by screening to eliminate multigrain particles and by washing to remove fine particles (Gray and Wilson 1995). Scanning electron microscopy (SEM) was used to confirm that the test specimens indeed consisted predominantly of individual grains.

The much coarser "particle" specimens used in the tests described in Section 3.3 were prepared by crushing and screening the de-clad fuel to -10/+24 Tyler mesh, which resulted in multigrain particles 700 to 1700 μm in size. A portion of these particles was oxidized in air at 175°C to form an oxide of approximate stoichiometry $\text{UO}_{2.4}$ as determined by weight-gain measurements (Einziger et al. 1992). Ceramographic and x-ray diffraction analyses showed that the material was U_4O_{9+x} containing small UO_2 remnants (~1 to 5 vol %) at the grain centers, and no detectable U_3O_8 or other oxidation products.

Surface areas of the grain-size powder specimens were determined using a method described by Brunauer, Emmett, and Teller (1938) (BET method). Surface areas of the particle specimens were determined by weighing a representative number (~50) of individual particles and calculating the surface area assuming that the particles were cubical in shape.^(a) This calculated area was multiplied by a somewhat arbitrarily chosen roughness factor of three to give what is considered to be a rough geometric surface area.

There is a very important difference in the relevance of the surface areas measured for these two very different types of test specimens by these two methods. The BET measurements made on the grain-size powder specimens are thought to provide a good measure of the actual area

(a) The particular geometry assumed is relatively unimportant for these calculations where surface area uncertainties of $\pm 50\%$ are considered acceptable. For example, the surface area of a cube is only 26% less than that of a 4 x 4 x 1 parallelepiped or 24% larger than that of a sphere, all of the same mass.

contacted by the water in the flowthrough tests. In contrast, the rough geometric surface areas determined for the particle specimens are known to be a poor representation of the area contacted by the water because the roughness factor of three accounts only for surface roughness, but does not account for partial penetration of water into the grain boundaries. The problem is intractable because there is no known way to measure the surface areas of particle specimens in a way that properly accounts for the water penetration into the grain boundaries. The rough geometric measurement obviously underestimates the effective surface area. On the other hand, a BET measurement would overestimate the effective surface area because the gas used to make the measurement penetrates much further into the grain boundaries than the water does. This problem is circumvented with the grain-size powder specimens because the powder consists predominantly of individual grains as confirmed by SEM examination. As a result, all or most of the grain boundaries are openly exposed to the water, which means that there are no occluded grain boundaries as there are in the particle specimens.

As a result of the inability to accurately measure the effective surface area of multigrain particle specimens, intrinsic dissolution rates cannot be measured using this type of specimen. However, *apparent* dissolution rates measured for particle specimens can be used to estimate the depth of water penetration into grain boundaries as discussed in Section 3.3.

3.0 Results and Discussion

The results of recent dissolution-rate tests are shown in Figures 1 to 12. The figures also show average dissolution rates, plus/minus one standard deviation, based on the U data as well as the time periods over which the data were averaged. Table 1 lists some of the characteristics of the spent fuels that have been tested while Tables 2 to 4 summarize some of the results from previous tests as well as the data provided in Figures 1 to 12.

The dissolution rate that is quoted as an average depends on the time period over which it is calculated, which is somewhat arbitrary. Therefore, there may be slight differences between the average values shown in the figures and in Tables 2 and 3, compared with averages that were based on these same data, but were cited in other sources, such as monthly or annual reports or various presentations.

The dissolution rates given in the figures and in Tables 2 and 3 were derived from the measured flow rates and component concentrations in the specimen cell effluent based on Equation (1). Dissolution rates in an earlier publication (Steward and Gray 1994) were based on Equation (2). For U, these two equations give values that differ by factors of 0.88 and 0.84, which represent the fractions of U in UO_2 and in ATM-103 spent fuel (see Table 3), respectively.

$$R = \frac{C_i F}{MAF_i} \quad (1)$$

$$R_i = \frac{C_i F}{MA} \quad (2)$$

where R = dissolution rate of the spent fuel matrix based on the data for component i (e.g., U, ^{137}Cs , ^{99}Tc , or ^{90}Sr) ($\text{mg}\cdot\text{m}^{-2}\cdot\text{d}^{-1}$)

R_i = dissolution rate of component i (e.g., U, ^{137}Cs , ^{99}Tc , or ^{90}Sr) ($\text{mg}\cdot\text{m}^{-2}\cdot\text{d}^{-1}$ or $\text{Bq}\cdot\text{m}^{-2}\cdot\text{d}^{-1}$)

C_i = concentration of component i in specimen cell effluent (mg/mL or Bq/mL)

F = flow rate of test solution through specimen cell (mL/d)

M = mass of test specimen (mg)

A = specific surface area of test specimen (m^2/mg)

f_i = concentration of component i (U, ^{137}Cs , ^{99}Tc , or ^{90}Sr) in test specimen (mg/mg or Bq/mg).

It is important to understand the implications of these equations. Equation (1) has the very distinct advantage that spent-fuel dissolution rates calculated from data for different components are equal if the specimen dissolves congruently. However, the calculated rate must not be interpreted to mean that R milligrams of *component i* are dissolving per unit surface area per day. Rather, the correct interpretation is that R milligrams of *spent fuel* are dissolving per unit surface area per day, based upon the data for component i .

The correct interpretation of Equation (2) is that R_i milligrams or becquerel of *component i* are dissolving per unit surface area per day. This is quite different from the amount of *spent fuel* that is dissolving, particularly when the component being considered has a low concentration in the fuel, e.g., ^{137}Cs . Equation (2) gives a direct and unambiguous value for the dissolution rates for the different components, but the rates for the different components will be very different simply because their concentrations in the fuel are very different. Therefore, they are difficult to present on a single graph. Furthermore, results calculated using Equation (2) do not indicate whether the spent fuel specimen is dissolving congruently. Finally, no matter whether Equation (1) or (2) is used to represent the data, the radioactive decay of any non-uranium

radionuclide being considered must be taken into account when applying the data (e.g., in a performance-assessment calculation).

The following subsections provide brief discussions on matrix dissolution rates, fission-product dissolution rates, and dissolution rates of oxidized fuels. These are followed by a discussion of results on ^{129}I gap inventories and a final subsection that discusses some apparent inconsistencies in Tc dissolution rate results for different test specimens and fuels.

3.1 UO_2 Matrix Dissolution Rate Tests as a Function of Burnup and Test Condition

Table 2 lists dissolution rates for several spent fuels. It shows that, over the range of conditions tested, fuels with burnups ranging from 30 to 50 MWd/kgM dissolved at approximately the same rate for a given test condition. The biggest difference between different fuels shown in Table 2 is for the test condition with $2 \times 10^{-2} \text{ M}$ carbonate at 75°C where the measured values for ATM-105 and ATM-106 were considerably less than the calculated value for ATM-103. This suggests that the equation used to generate the calculated values (Steward and Gray 1994) may err on the high side for this test condition.

Data in Table 2 represent burnups only between 30 and 50 MWd/kgM. To extend the burnup coverage, fuel with 13 MWd/kgM burnup is currently being tested, and fuel with ~65 MWd/kgM burnup has been acquired and will be tested in the near future.

3.2 Fission Product Dissolution Rates

All 12 figures contain data for ^{137}Cs , ^{99}Tc , and ^{90}Sr as well as for U. For grain-size powder specimens, which are represented in all Figures except 10 and 12, it was expected that these elements would dissolve congruently with the U except, perhaps, for an initial transient period. This expectation was based on the knowledge that, for this type of test specimen, essentially all of the grain boundaries were exposed directly to the water. As a result, any Cs or other element that

may have been concentrated at the grain boundaries would have quickly dissolved. Subsequently, all elements would be expected to dissolve congruently with the U because all are controlled by the rate of dissolution of the UO_2 matrix.

In agreement with this expectation, approximately congruent dissolution has generally been observed in previous tests with grain-size powder specimens of spent fuel (Gray and Strachan 1991; Gray and Wilson 1995). Congruency was also generally observed with the ATM-105 fuel in Figures 1 to 3. However, the Cs and Tc data for ATM-105 fuel in Figure 4 are up to about 50% higher than the U rates. Since the test specimen in each of the four tests was simply a portion of the same batch of test material, the inconsistency cannot be attributed to a difference in test specimens and must be viewed with reservation.

Data for ATM-106 fuel represented in Figures 5 to 8 show that the Cs dissolved somewhat faster than the U under all four test conditions. Although the difference between the Cs and U gradually decreased throughout each test, the Cs rate remained somewhat higher than the U even after 73 days of testing. All Cs concentrated at the grain boundaries would have been expected to dissolve almost immediately at the start of each test for the reason described above. Therefore, the high Cs results may indicate a Cs concentration gradient between the grain peripheries and grain centers as was suggested in a previous study (Gray and Strachan 1991).

The Tc and Sr data are congruent with the U data in Figures 5 to 7, but the Tc data are a little high and the Sr data are a little low in Figure 8. This is the same test condition where the Cs and Tc data were found to be somewhat incongruent with U for the ATM-105 fuel in Figure 4. However, it seems unlikely that slightly incongruent dissolution would be a repeatable result of this test condition and, again, must be viewed with caution.

3.3 Dissolution Rate Tests with Oxidized Fuels

Figures 9 to 12 show results for unoxidized (UO_2) and oxidized (U_4O_{9+x}) ATM-104 spent fuel grains ($\sim 12 \mu\text{m}$) and multigrain particles (700 to 1700 μm) prepared using the same methods described previously (Gray and Wilson 1995). Table 3 lists the average steady-state dissolution

rates, which were based on the U results, for the ATM-104 fuel specimens along with results obtained previously with ATM-105 and ATM-106 fuels.

Note that the test conditions for ATM-105 were different from those used with the ATM-104 and ATM-106 fuels. This precludes a direct comparison between ATM-105 and the other two fuels. However, the purpose of the tests in each case was to compare results for oxidized versus unoxidized specimens, not for comparison between different fuels. The tests with ATM-105 were conducted first, and a decision was made after that to change the conditions for future tests. The new test condition (2×10^{-2} M total carbonate, pH =8, 25°C, atmospheric oxygen partial pressure), which will be included in most future testing to allow a wider variety of direct comparisons between different fuels, was used in the tests with oxidized and unoxidized specimens of ATM-104 and ATM-106 fuels.

Oxidation has the potential to change spent-fuel dissolution rates in two ways. First, it could change the intrinsic dissolution rates.^(a) Second, it could increase the dissolution rate of fuel particles by making the grain boundaries more accessible to the water, thereby increasing the effective surface area. Table 3 shows that the intrinsic dissolution rates of ATM-104 and ATM-105 (data obtained using grain specimens) were not significantly affected by oxidation, but there was a modest increase in the intrinsic dissolution rate of ATM-106 fuel grains.

Tests conducted with multigrain particles (Figures 10 and 12) allow the extent of grain-boundary penetration by the test solution to be estimated by comparing the dissolution rates of the particles with those obtained using grain-size powder specimens (Figures 9 and 11). Gray and Wilson (1995) described the method used to estimate the grain-boundary penetration. Briefly, it is based on the belief that the intrinsic dissolution rate of both grains and particles must be the same. The particles only *appear* to dissolve faster because the surface areas used to normalize the data do not adequately account for partial penetration of water into the grain boundaries. This

(a) Dissolution rates measured for grain specimens are considered to be intrinsic because they are not obscured by uncertainty about the degree of grain-boundary penetration by the water and the resultant uncertainty about the effective surface area. See the description of grain specimens in Section 2.0.

apparent difference was used to estimate the extent of grain-boundary penetration listed in Table 3.

Oxidation left the dissolution rate of ATM-105 particles unchanged, which implies that the depth of water penetration into the grain boundaries was unchanged by the oxidation. In contrast to the ATM-105 particles, oxidation had a marked effect on the dissolution rates of ATM-104 and ATM-106 particles. This effect can be attributed to opening of the grain boundaries by the oxidation, which allows greater water penetration, thereby increasing the effective surface area available for reaction with the water. So great was this effect with ATM-104 that the water appears to have penetrated the entire volume of grain boundaries throughout the particles. This is evident from the estimated depth of water penetration (~100 grain layers) multiplied by the grain size (~12 μm), which leads to a penetration depth that is well over half the particle diameters (700 to 1700 μm).

Because replicate tests have not been run, it is not possible to say whether particle specimens of the three different fuels in Table 3 really respond differently to oxidation and subsequent reaction with water or if the observed differences were simply sample-to-sample variations. However, the data do suggest that oxidation up to the U_4O_{9+x} stage does not have a large effect on the intrinsic dissolution rates, which were obtained with grain-size powder specimens (the largest increase was a factor of <6).

Data for the particle specimen of ATM-104 fuel, in particular, suggest that the extent of oxidation represented here could markedly increase dissolution rates of relatively intact fuel rods by opening the grain boundaries and thereby increasing the effective surface area that is available for contact by water. From a disposal viewpoint, this is a potentially important consideration, even though intrinsic dissolution rates have not been found to be markedly affected by oxidation to the U_4O_{9+x} stage.

3.4 ^{129}I Gap Inventories

The inventories of ^{129}I contained in the gap regions of a few different fuel rods were measured using a slight variation on a method developed by Stroes-Gascoyne et al. (1995). Inch-long segments of fuel were pressed out of the cladding, and the fuel plus the cladding was placed in a beaker with 250 mL of borated buffer (pH = 8.5) containing 20 mg/L of KI as iodine carrier. After standing for 24 hours,^(a) an aliquot of the solution was filtered (0.45 μm) and analyzed for concentrations of the ^{127}I carrier (to determine recovery efficiency which ranged from 64 to 100%) and ^{129}I using inductively coupled plasma/mass spectrometry (ICP/MS). The results shown in Table 4 are for two sets of measurements on different specimens conducted a few months apart. Agreement between the two sets of measurements (within a factor of about 2) is fairly typical for these types of tests.

The data in Table 4 show that the ^{129}I gap inventories are substantially less than the fission gas release (FGR), except for the fuel with the highest FGR. This contrasts with results for CANDU (CANada Deuterium Uranium) fuel (Stroes-Gascoyne et al. 1995) where a more nearly one-to-one correlation was found for fuels with linear power rates <42 kW/m. None of the fuels listed in Table 4 had power rates above 30 kW/m, which would put them in the same category with the CANDU fuels where the one-to-one correlation between FGR and ^{129}I gap inventory was found. However, U.S. LWR and CANDU fuels differ significantly in burnup with the latter being only about 10 MWd/kgM, which could turn out to be important from the standpoint of ^{129}I gap inventories. It should also be noted that a general correlation between FGR and ^{129}I gap inventories is not yet available for LWR fuels because only a limited number have been tested to date.

(a) Earlier tests conducted over a period of one week showed that 24 hours was sufficient to dissolve the ^{129}I gap inventory.

3.5 Tc Dissolution Rates

The Tc results from the various flowthrough tests have been an enigma. For example, Figures 9 and 11 show that, following the initial transient, the Tc dissolved only about half as fast as U from both oxidized and unoxidized specimens of ATM-104. In previous tests, similar behavior was observed with ATM-106, but the Tc and U dissolved nearly congruently from both oxidized and unoxidized specimens of ATM-105 (Gray and Thomas 1994). The fact that Tc dissolves slower than the UO_2 matrix in some cases may be related to the fact that some of the Tc is present as one of the constituents of the so-called 5-metal particles (Thomas and Guenther 1988, Thomas and Charlot 1990), which may dissolve more slowly than the matrix. Complicating the issue is the fact that the distribution and size of the Tc-bearing 5-metal particles varies from fuel to fuel in ways that appear to be related to burnup and temperature distribution in the fuel. The variation in the Tc distribution may contribute to the variation in the Tc-dissolution data that have been observed. However, an explanation for these observations that is consistent with what is known about the condition of the Tc in the fuel has not been formulated.

4.0 References

- Brunauer, S, P Emmett, and E Teller. 1938. "Adsorption of Gases in Multimolecular Layers," *J. Am. Chem. Soc.* 60:309-319.
- Einzig, RE, LE Thomas, HC Buchanan, and RB Stout. 1992. "Oxidation of Spent Fuel in Air at 175 to 195°C." *J. Nucl. Mater.* 190:53-60.
- Gray, WJ, and LE Thomas. 1994. "Initial Results from Dissolution Testing of Various Air-Oxidized Spent Fuels." *Sci. Basis for Nucl. Waste Management XVII*. Vol. 333, ed. A. Barkatt and R. A. Van Konynenburg, pp. 391-398. Materials Research Society, Pittsburgh, Pennsylvania.
- Gray, WJ and CN Wilson. 1995. *Spent Fuel Dissolution Studies FY 1991 to 1994*. PNL-10540, Pacific Northwest National Laboratory, Richland, Washington.
- Gray, WJ, and DM Strachan. 1991. "UO₂ Matrix Dissolution Rates and Grain-Boundary Inventories of Cs, Sr, and Tc in Spent LWR Fuel." *Sci. Basis for Nucl. Waste Management XIV*. Vol. 212, ed. T. A. Abrajano, Jr. and L. H. Johnson, pp. 205-212. Materials Research Society, Pittsburgh, Pennsylvania.
- Steward, SA and WJ Gray. 1994. "Comparison of U Dissolution Rates from Spent Fuel and Uranium Dioxide." *High-Level Radioactive Waste Management: Proceedings of the Fifth International Conference*. pp. 2602-2608. American Nuclear Society, Inc., La Grange Park, Illinois.
- Stroes-Gascoyne, S, DL Moir, MKolar, RJ Porth, JL McConnell, and AB Kerr. 1995. "Measurement of Gap and Grain-Boundary Inventories of ¹²⁹I in Used CANDU Fuels." *Sci. Basis for Nucl. Waste Management XVIII*. Vol. 353, ed. T. Murakami and R. C. Ewing, pp. 625-631. Materials Research Society, Pittsburgh, Pennsylvania.
- Thomas, LE and RJ Guenther. 1988. "Characterization of Low-Gas-Release LWR Fuels by Transmission Electron Microscopy." *Sci. Basis for Nucl. Waste Management XII*. Vol. 127, ed. W. Lutze and R. C. Ewing, pp. 293-300. Materials Research Society, Pittsburgh, Pennsylvania.
- Thomas, LE and LA Charlot. 1990. "Analytical Electron Microscopy of Light-Water Reactor Fuels." *Ceramic Transactions* 9:397-407.

Table 1. Spent Fuel Characteristics

<u>Fuel</u>	<u>Rod</u>	<u>Grain Size (μm)</u>	<u>Reactor Type</u>	<u>Peak Burnup (MWd/kgM)</u>	<u>Fission Gas Release (%)</u>
ATM-103	MLA-098	14-22	PWR	30	0.25
ATM-104	MKP-109	9-14	PWR	44	1.1
ATM-105	ADD-2974	11-15	BWR	31	0.59
ATM-105	ADD-2966	15-28	BWR	34	7.9
ATM-106	NBD-095	NM ^(a)	PWR	43	7.4
ATM-106	NBD-107	7-16	PWR	46	11
ATM-106	NBD-131	NM ^(a)	PWR	50	18

a) not measured

Table 2. Dissolution Rate ($\text{mg}\cdot\text{m}^{-2}\cdot\text{d}^{-1}$)^(a) of Spent Fuel at pH = 8 and Atmospheric Oxygen Partial Pressure

Fuel	Burnup (MWd/kgM)	FGR (%)	Surface Area (cm^2/g)	2×10^{-2} M Carbonate ^(b)				2×10^{-4} M Carbonate ^(b)			
				25°C		75°C		25°C		75°C	
				Meas.	Calc. ^(c)	Meas.	Calc. ^(c)	Meas.	Calc. ^(c)	Meas.	Calc. ^(c)
ATM-103 ^(d)	30	0.25	860	4.1	5.1		31		1.8	10	11
ATM-104 ^(e)	44	1.1	1360	3.5							
ATM-105 ^(f)	31	0.59	680	4.0		9.1		2.6		11	
ATM-106 ^(d)	50	18	2770	1.5							
ATM-106 ^(g)	50	18	1020	3.8		6.9		2.9		9.5	

a) Based on U data

b) Test solutions made up of appropriate concentrations of NaHCO_3 and Na_2CO_3 and sparged with air containing suitable concentrations of CO_2 to maintain pH = 8

c) Calculated using an equation derived by Steward and Gray (1994) for ATM-103 spent fuel at atmospheric oxygen partial pressure

d) Data from Gray and Wilson (1995)

e) Data from Figure 9

f) Data from Figures 1 to 4

g) Data from Figures 5 to 8

Table 3. Dissolution Rate ($\text{mg}\cdot\text{m}^{-2}\cdot\text{d}^{-1}$)^(a) and Estimated Grain Boundary Penetration of Unoxidized (UO_2) and Oxidized (U_4O_{9+x}) Spent Fuel

Fuel	Rod	Unoxidized			Oxidized		
		Grains	Particles	GBP ^(b)	Grains	Particles	GBP ^(b)
ATM-104 ^(c, e)	MKP-109	3.5	35	4-6	3.2	164	~100
ATM-106 ^(c, f)	NBD-131	1.5	25	6-9	8.2	241	12-18
ATM-105 ^(d, f)	ADD-2974	6.6	25	2-3	7.4	28	2-3

a) Based on U data

b) Grain Boundary Penetration. Estimate of depth of water penetration into the grain boundaries (number of grain layers)

c) 2×10^{-2} M total carbonate, pH =8, 25°C, atmospheric oxygen partial pressure

d) 2×10^{-3} M total carbonate, pH =9, 50°C, atmospheric oxygen partial pressure

e) Data taken from Figures 9-12

f) Data taken from Gray and Wilson 1995

Table 4. ^{129}I Gap Inventories of Different Spent Fuels

Fuel	Type	Fission Gas Release (%)	^{129}I Gap Inventory (%)	
			First	Second
ATM-105	BWR	0.59	<0.03	0.13
ATM-105	BWR	7.9	1.6	3.3
ATM-106	PWR	7.4	0.1	NM ^(a)
ATM-106	PWR	11	1.5	1.1
ATM-106	PWR	18	17	12

a) Not Measured

Pacific Northwest National Laboratory

Operated by Battelle for the
U.S. Department of Energy

March 2, 1999

To recipients of PNNL-11895:

Several months ago, you received a copy of PNNL-11895, *Spent Fuel Dissolution Rates as a Function of Burnup and Water Chemistry*, by W. J. Gray dated June 1998.

Unfortunately, an error was discovered in this document. The technetium (Tc) data in Figures 5 to 8, pages 21 to 24, are incorrect. Replacement figures, which show the corrected Tc data, are enclosed. No other data in this report were affected by this error.

Sincerely,



Walter J. Gray
Senior Scientist

enclosures (4)

902 Battelle Boulevard • P.O. Box 999 • Richland, WA 99352

Telephone: (509) 376-9693; e-mail: walt.gray@pnl.gov; Fax: (509) 376-9781

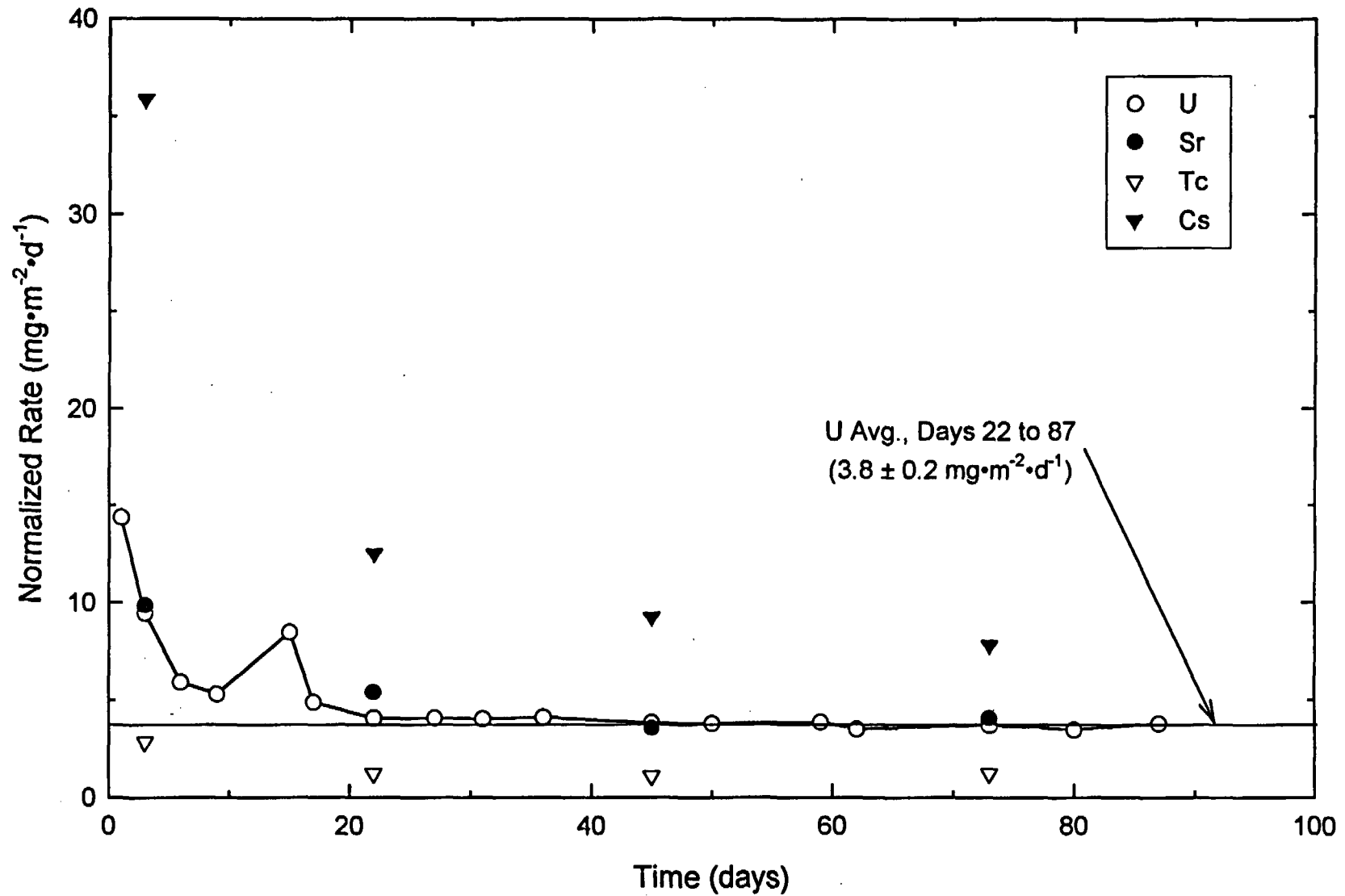


Figure 5. Dissolution Rate of ATM-106 Spent Fuel Grains in Aerated Water Containing $2 \times 10^{-2} \text{ M}$ Carbonate/Bicarbonate, pH = 8, at 25°C

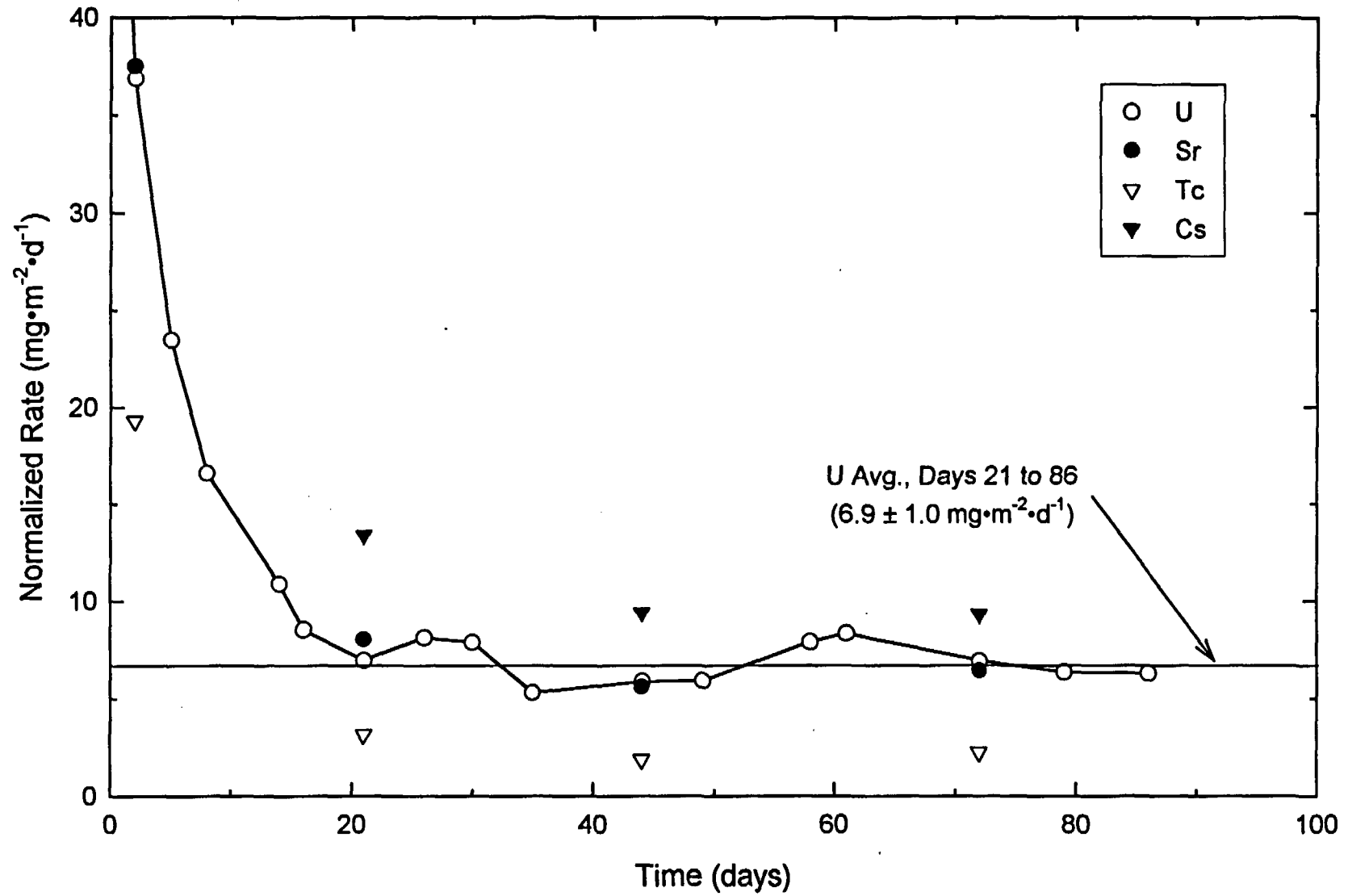


Figure 6. Dissolution Rate of ATM-106 Spent Fuel Grains in Aerated Water Containing $2 \times 10^{-2} \text{ M}$ Carbonate/Bicarbonate, $\text{pH} = 8$, at 75°C

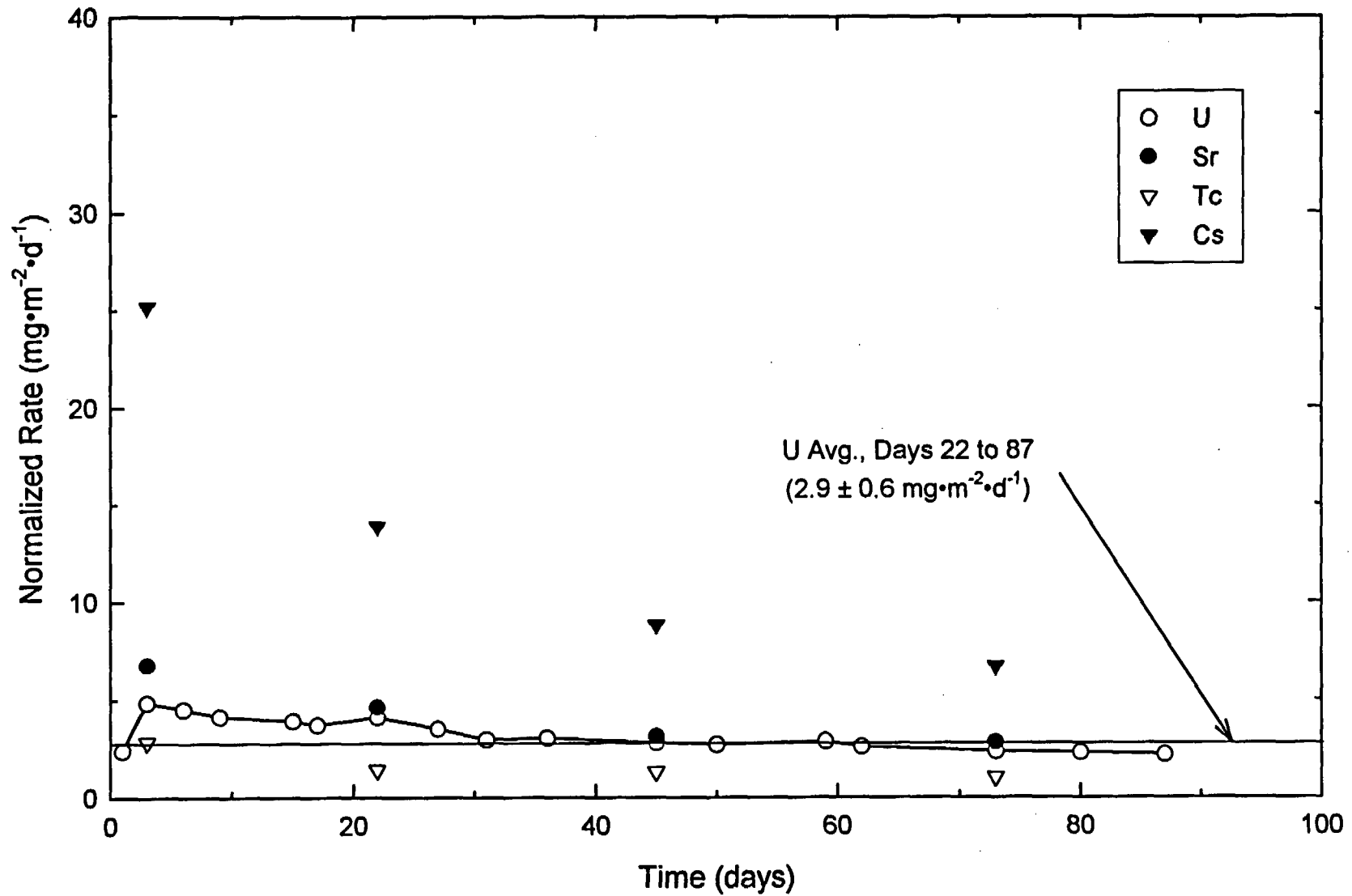


Figure 7. Dissolution Rate of ATM-106 Spent Fuel Grains in Aerated Water Containing $2 \times 10^{-4} \text{ M}$ Carbonate/Bicarbonate, $\text{pH} = 8$, at 25°C

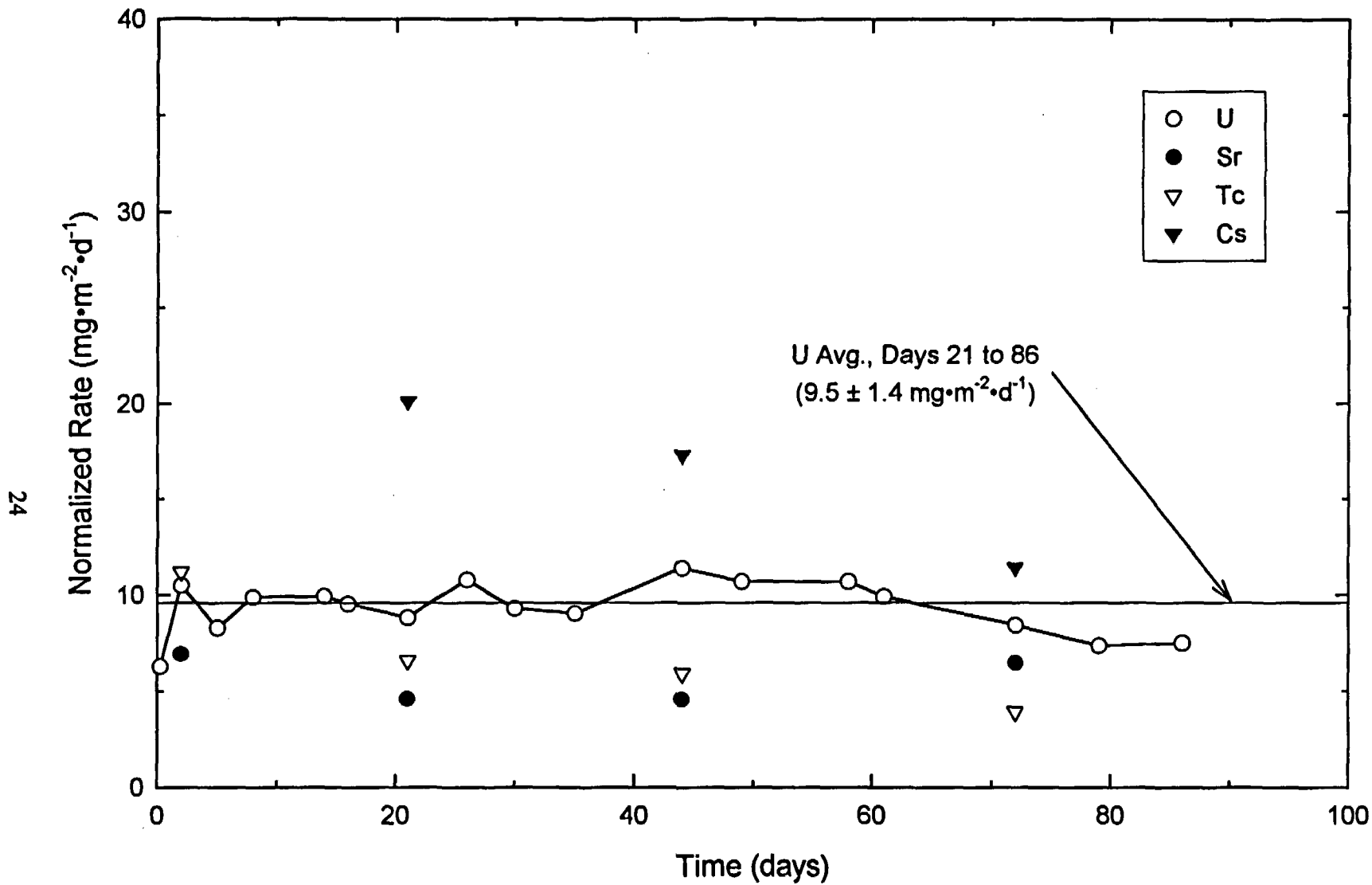


Figure 8. Dissolution Rate of ATM-106 Spent Fuel Grains in Aerated Water Containing $2 \times 10^{-4} \text{ M}$ Carbonate/Bicarbonate, pH = 8, at 75°C

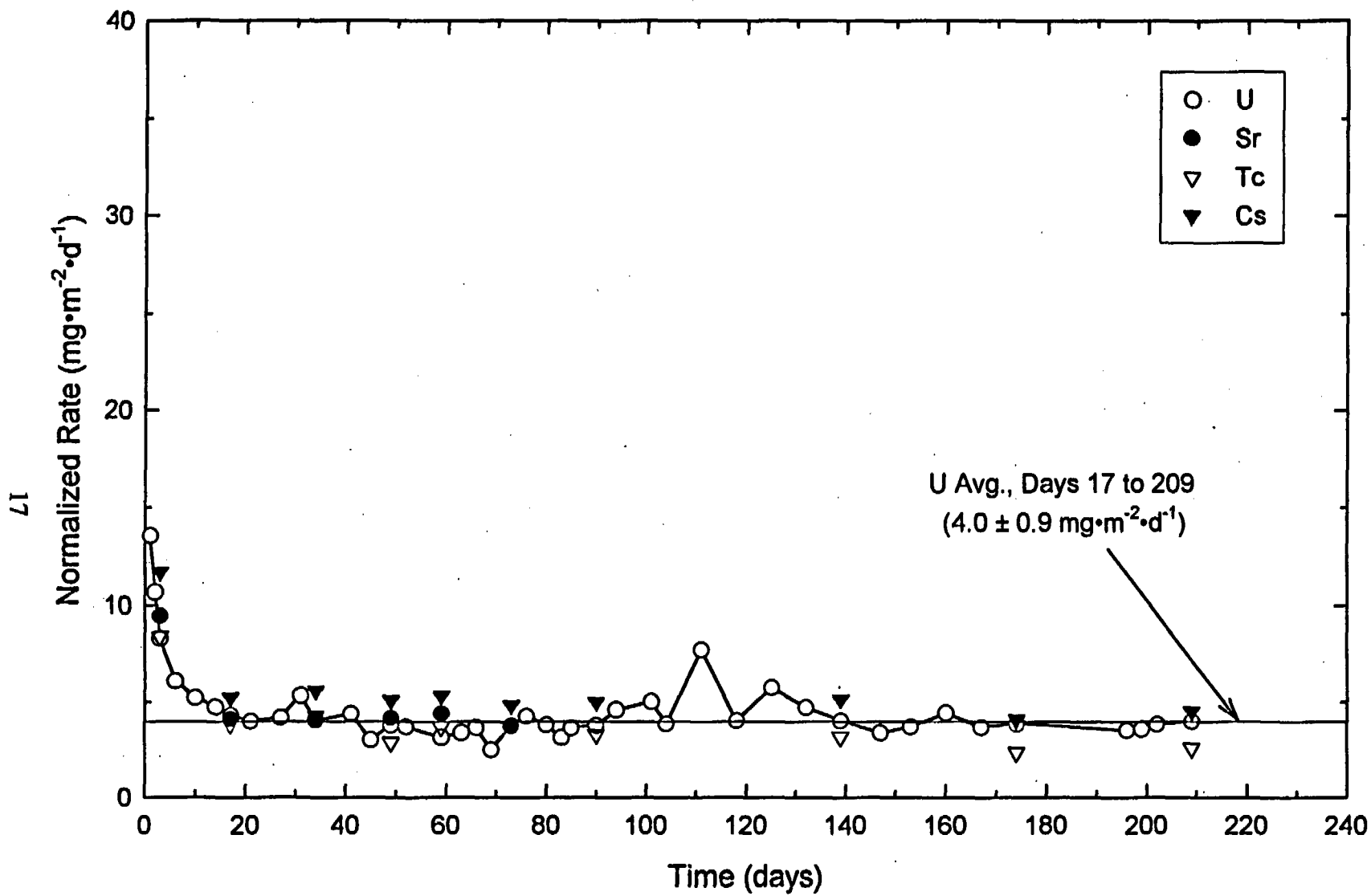


Figure 1. Dissolution Rate of ATM-105 Spent Fuel Grains in Aerated water containing $2 \times 10^{-2} \text{ M}$ Carbonate/Bicarbonate, pH = 8, at 25°C

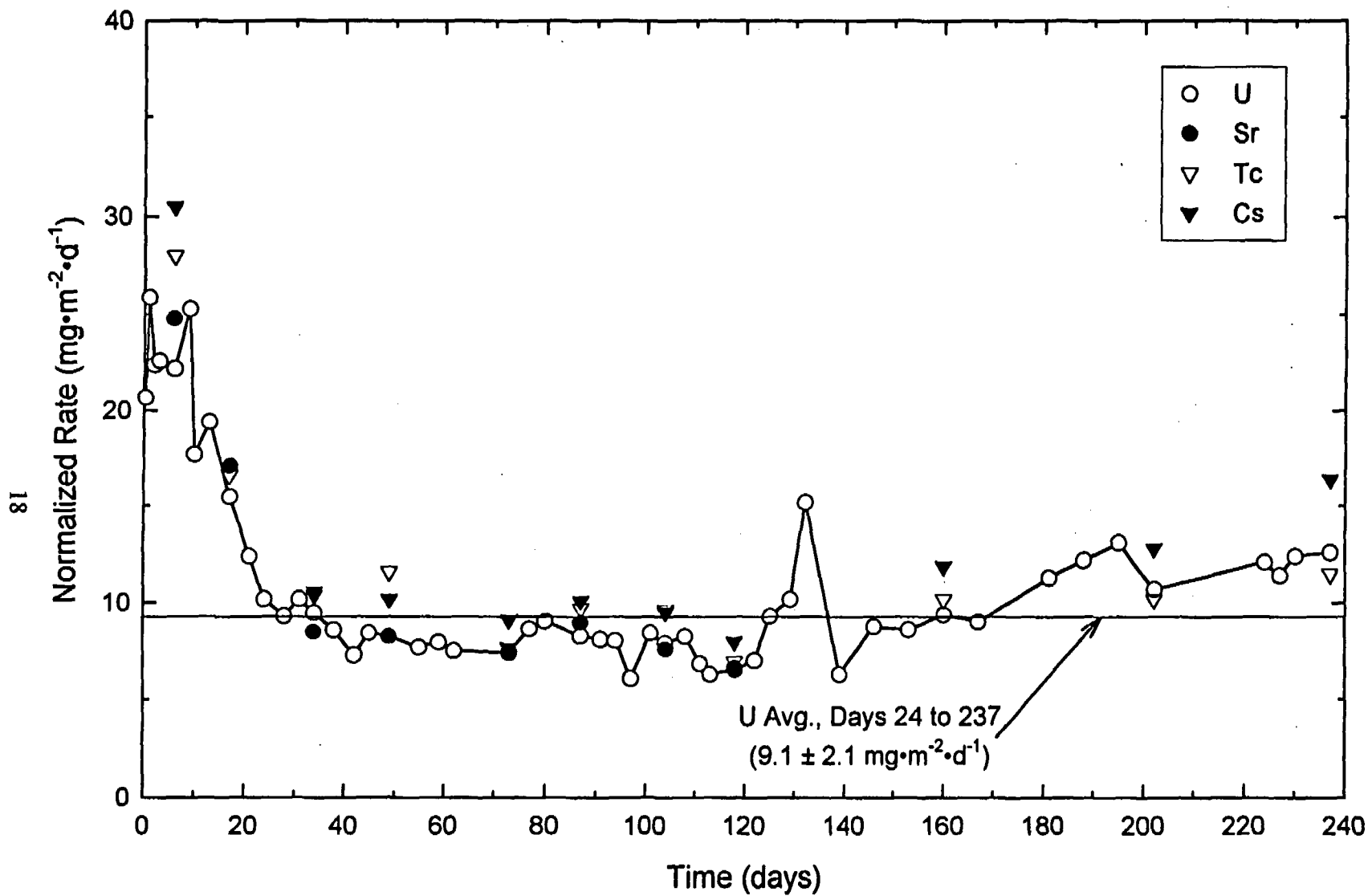


Figure 2. Dissolution Rate of ATM-105 Spent Fuel Grains in Aerated water containing $2 \times 10^{-2} \text{ M}$ Carbonate/Bicarbonate, pH = 8, at 75°C

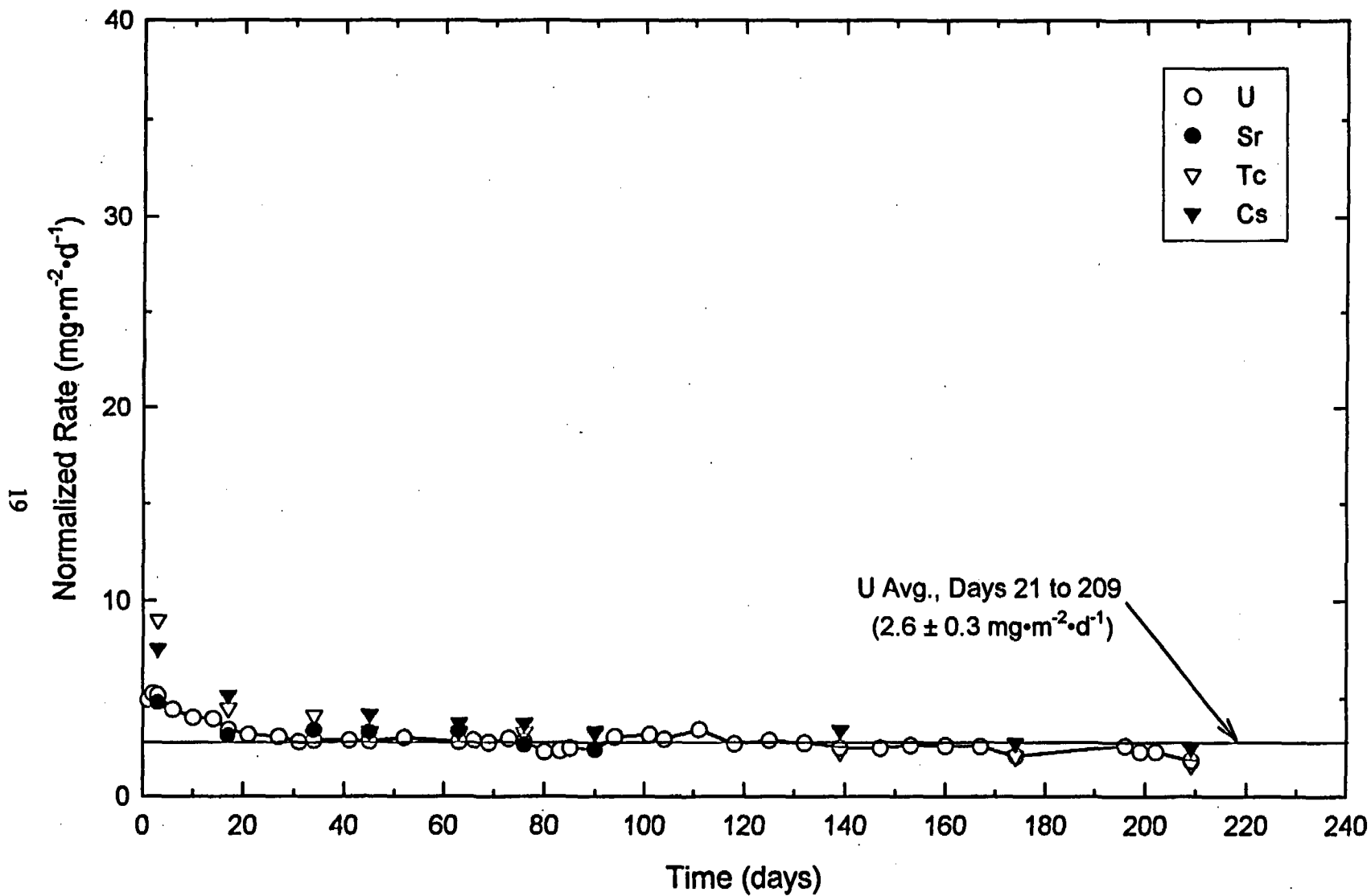


Figure 3. Dissolution Rate of ATM-105 Spent Fuel Grains in Aerated water containing $2 \times 10^{-4} \text{ M}$ Carbonate/Bicarbonate, pH = 8, at 25°C

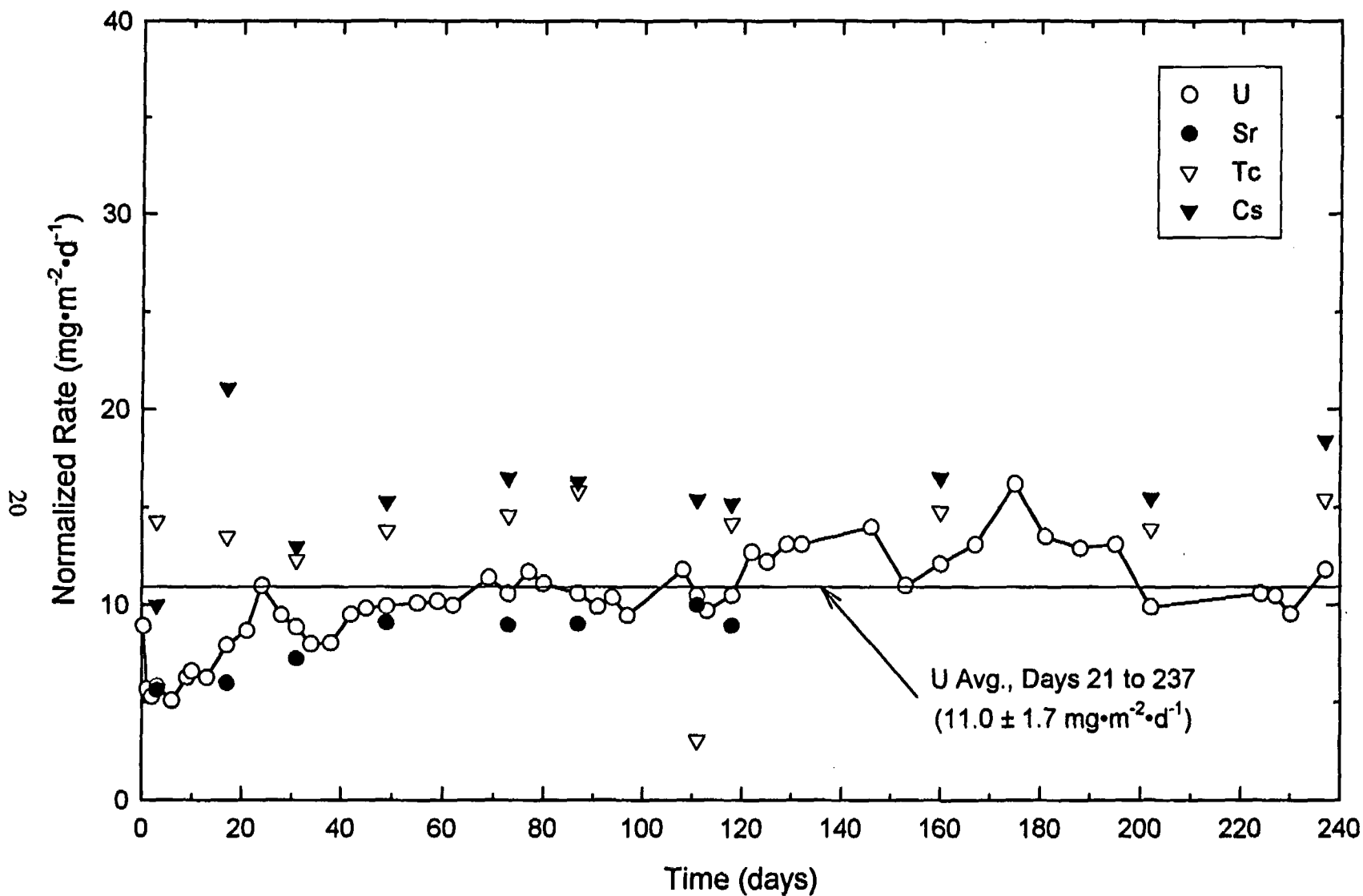


Figure 4. Dissolution Rate of ATM-105 Spent Fuel Grains in Aerated water containing $2 \times 10^{-4} \text{ M}$ Carbonate/Bicarbonate, pH = 8, at 75°C

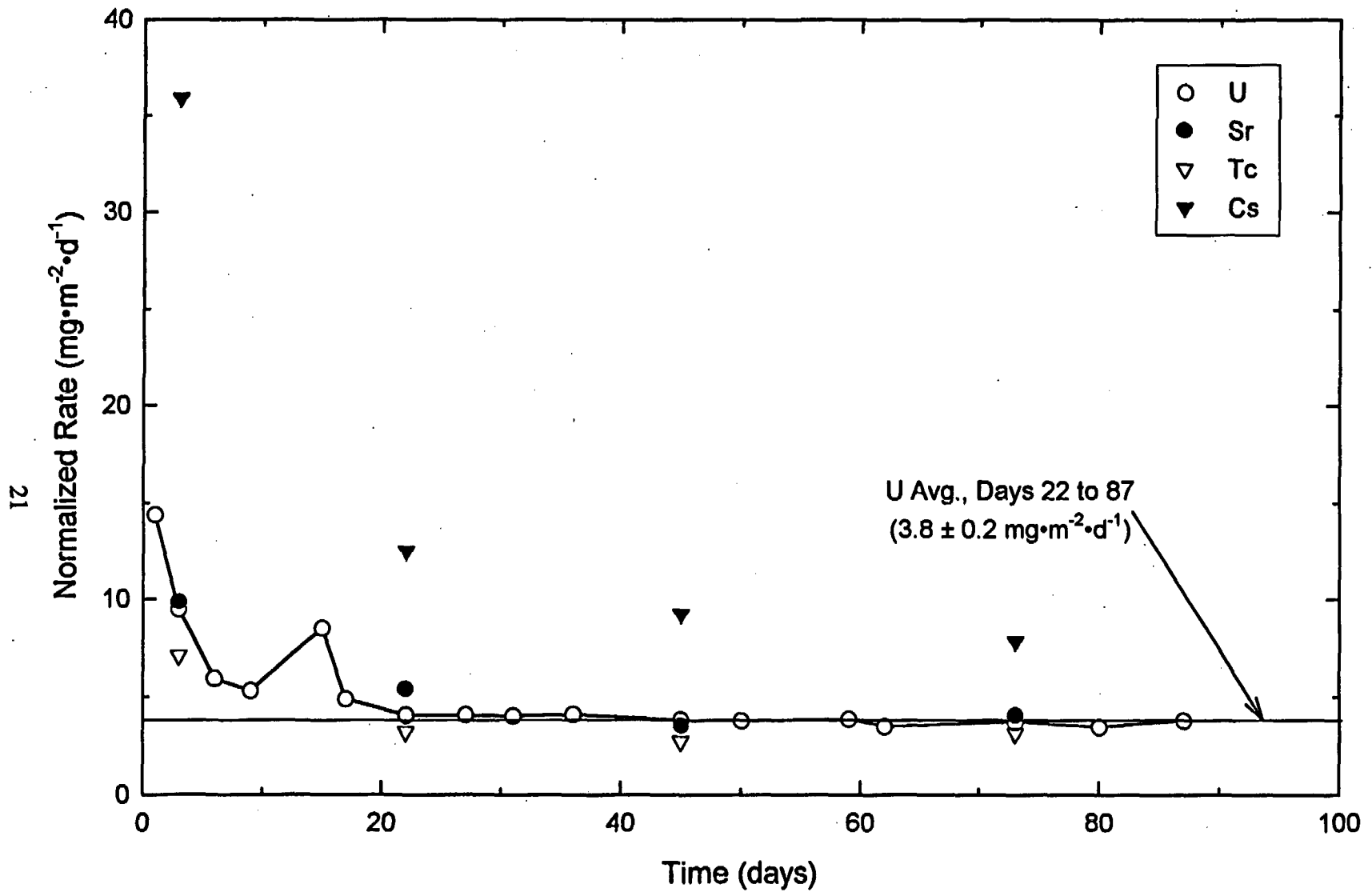


Figure 5. Dissolution Rate of ATM-106 Spent Fuel Grains in Aerated water containing $2 \times 10^{-2} \text{ M}$ Carbonate/Bicarbonate, pH = 8, at 25°C

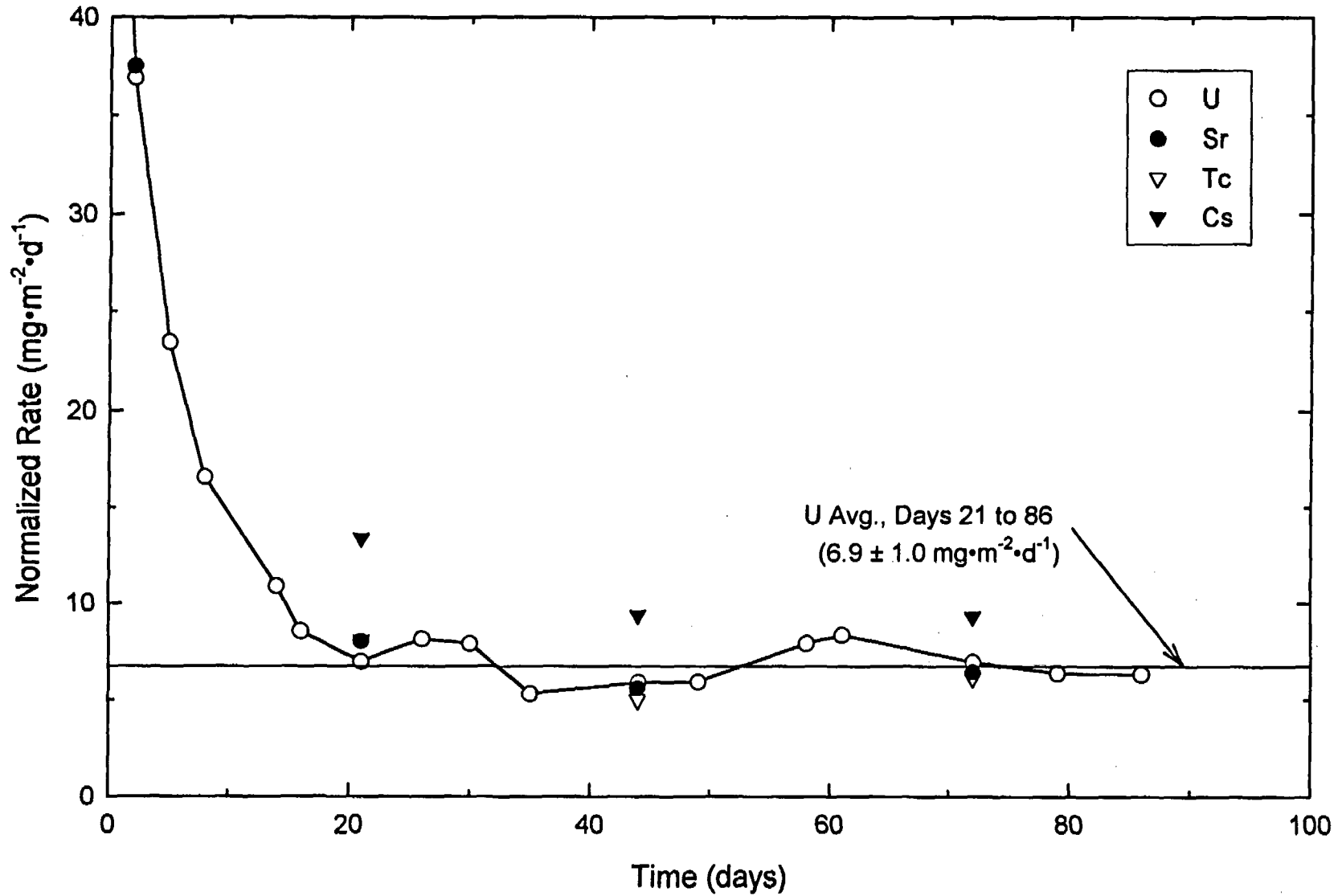


Figure 6. Dissolution Rate of ATM-106 Spent Fuel Grains in Aerated water containing $2 \times 10^{-2} \text{ M}$ Carbonate/Bicarbonate, pH = 8, at 75°C

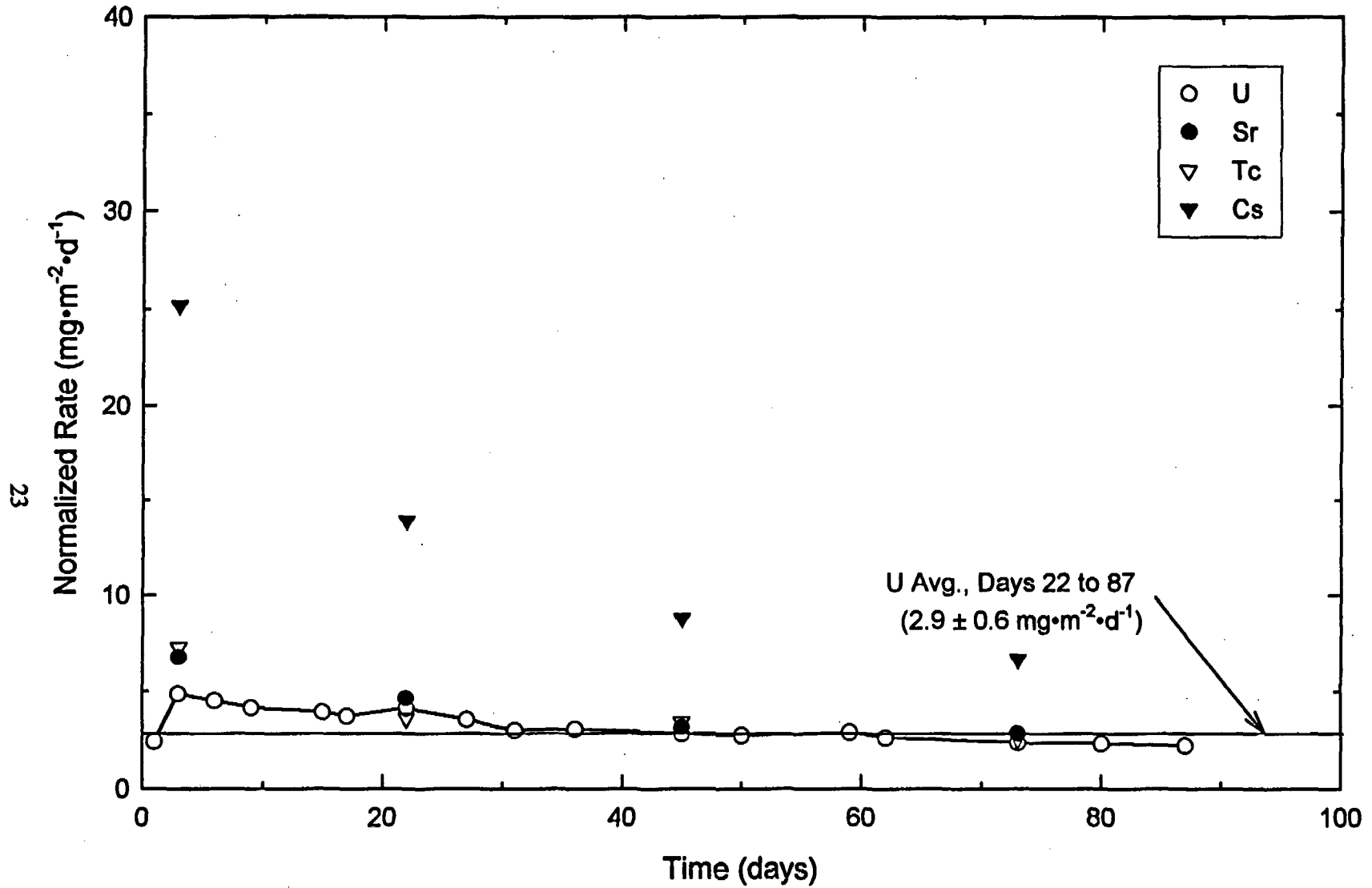


Figure 7. Dissolution Rate of ATM-106 Spent Fuel Grains in Aerated water containing $2 \times 10^{-4} \text{ M}$ Carbonate/Bicarbonate, pH = 8, at 25°C

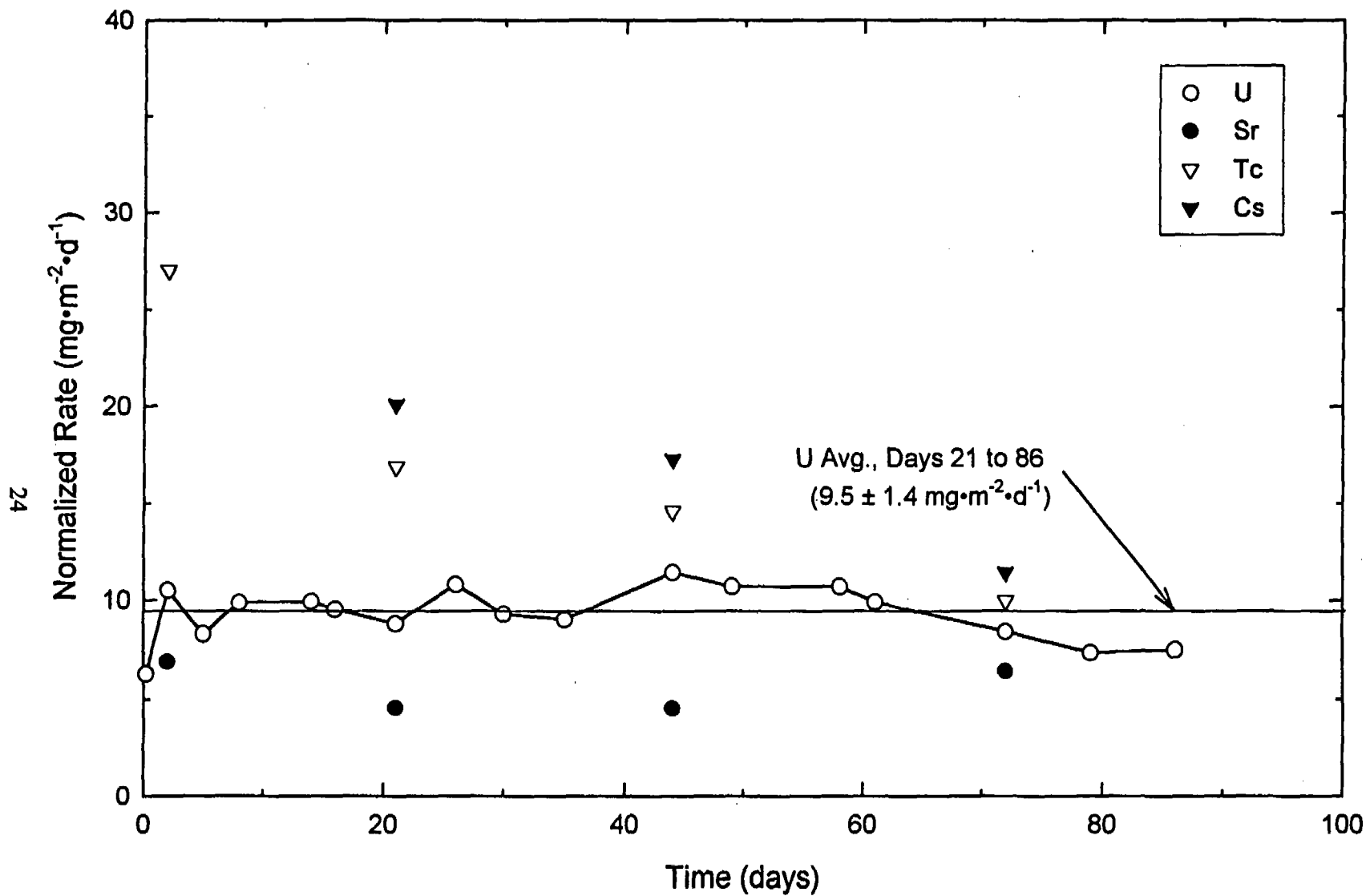


Figure 8. Dissolution Rate of ATM-106 Spent Fuel Grains in Aerated water containing $2 \times 10^{-4} \text{ M}$ Carbonate/Bicarbonate, $\text{pH} = 8$, at 75°C

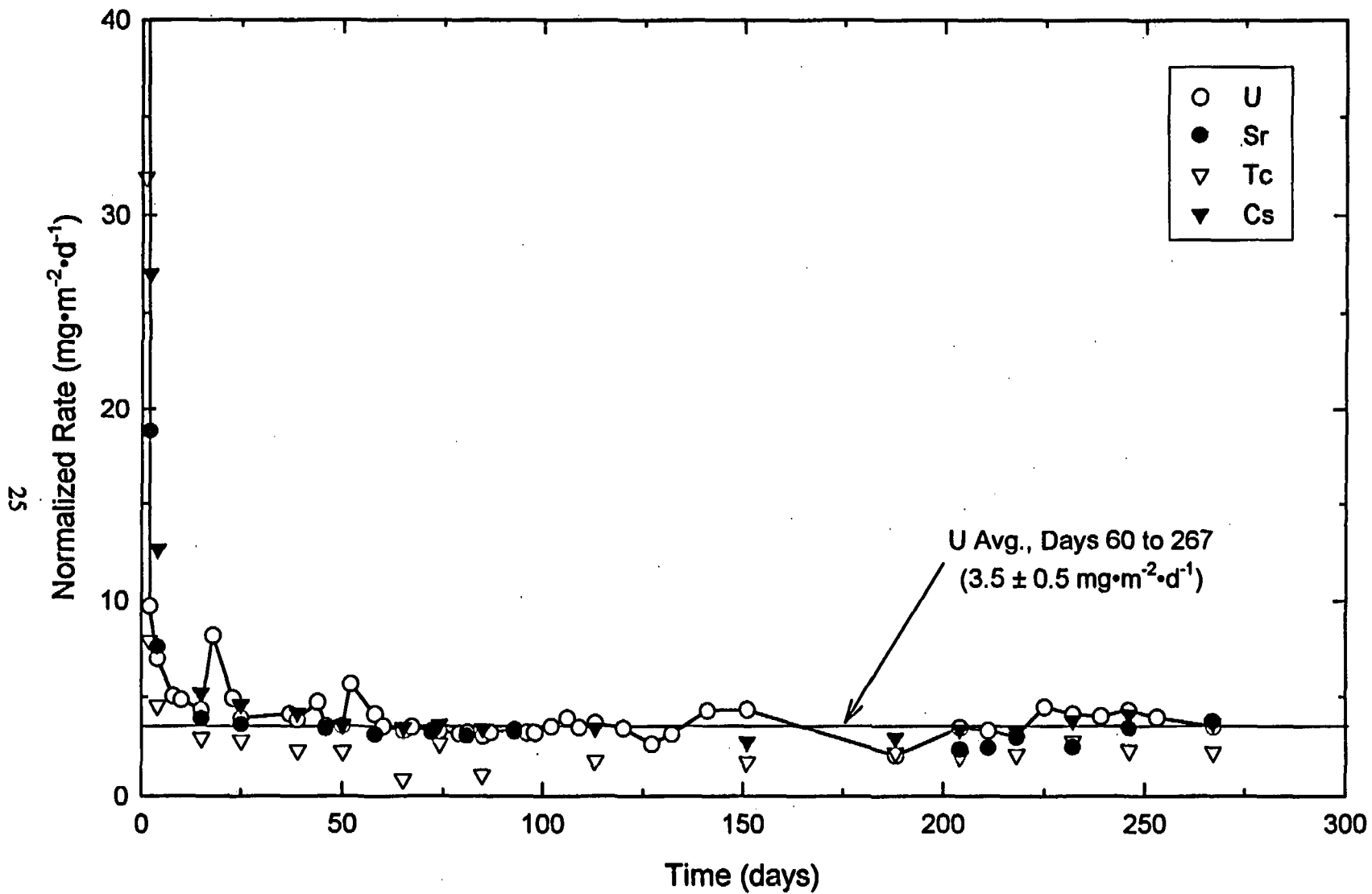


Figure 9. Dissolution Rate of Unoxidized (UO_2) Grains of ATM-104 Spent Fuel in Aerated Water Containing $2 \times 10^{-2} \text{ M}$ Carbonate/Bicarbonate, $\text{pH} = 8$, at 25°C

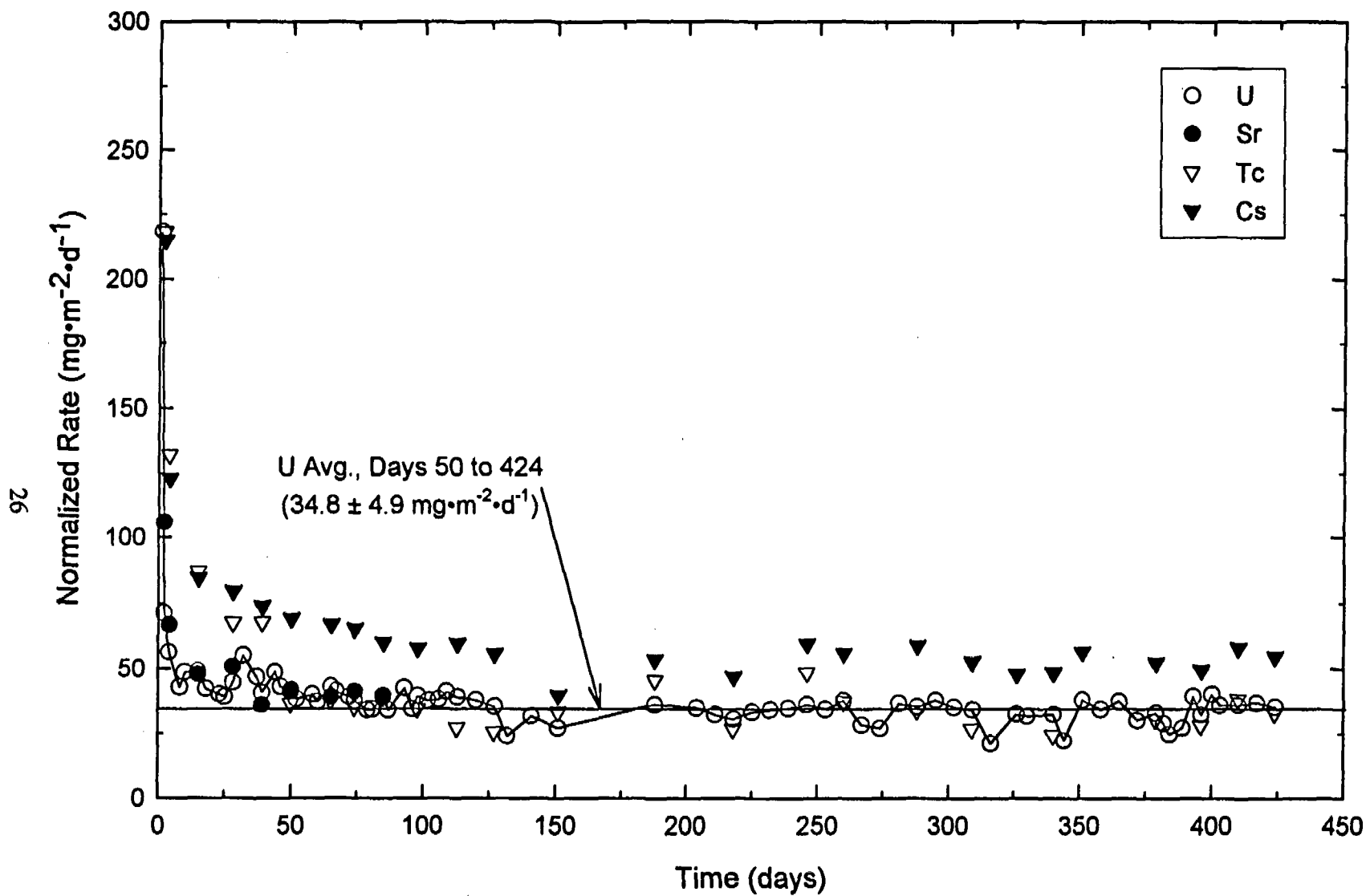


Figure 10. Dissolution Rate of Unoxidized (UO_2) Particles of ATM-104 Spent Fuel in Aerated Water Containing $2 \times 10^{-2} \text{ M}$ Carbonate/Bicarbonate, $\text{pH} = 8$, at 25°C

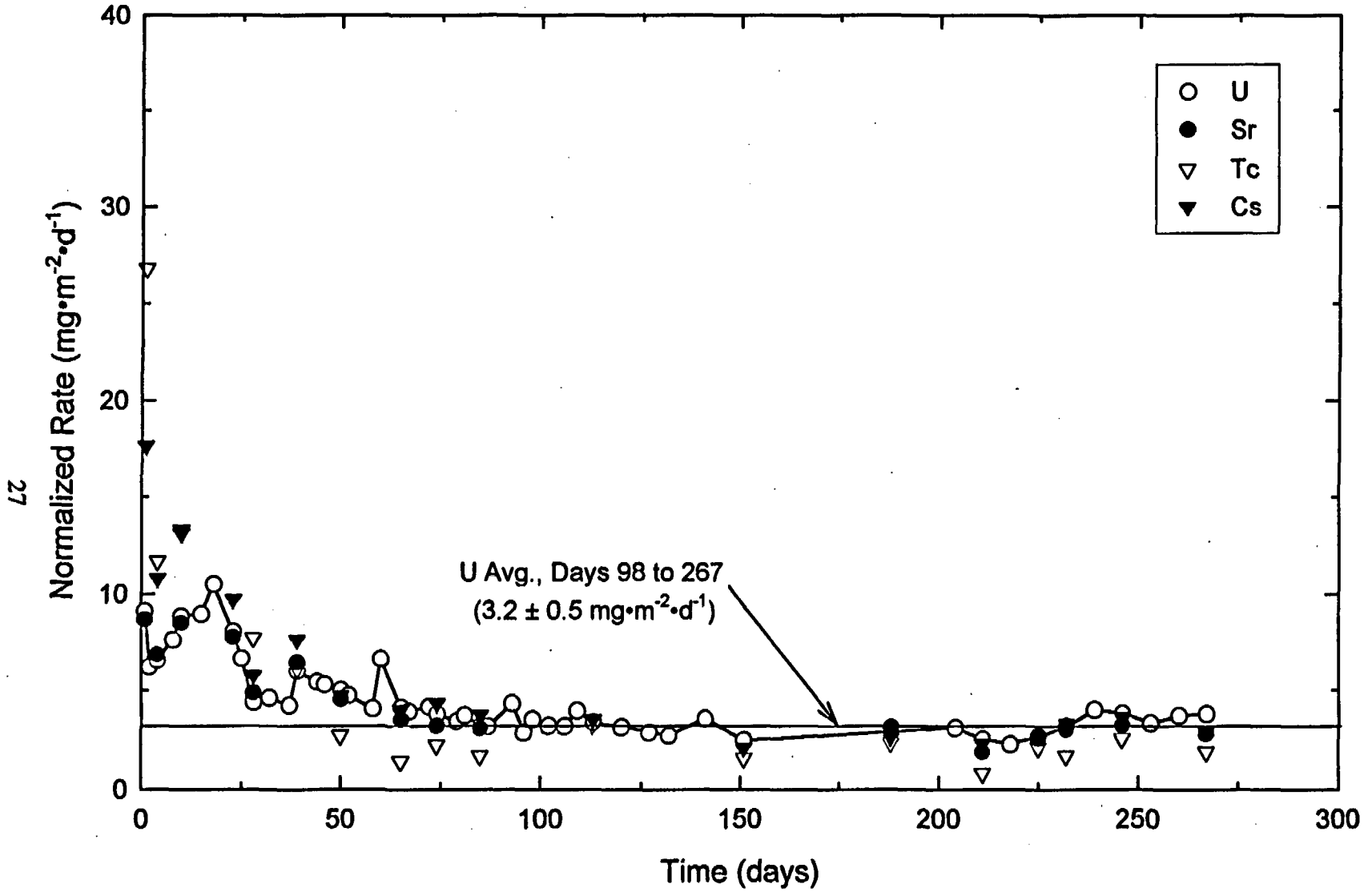


Figure 11. Dissolution Rate of Oxidized (U_4O_{9+x}) Grains of ATM-104 Spent Fuel in Aerated Water Containing $2 \times 10^{-2} \text{ M}$ Carbonate/Bicarbonate, $\text{pH} = 8$, at 25°C

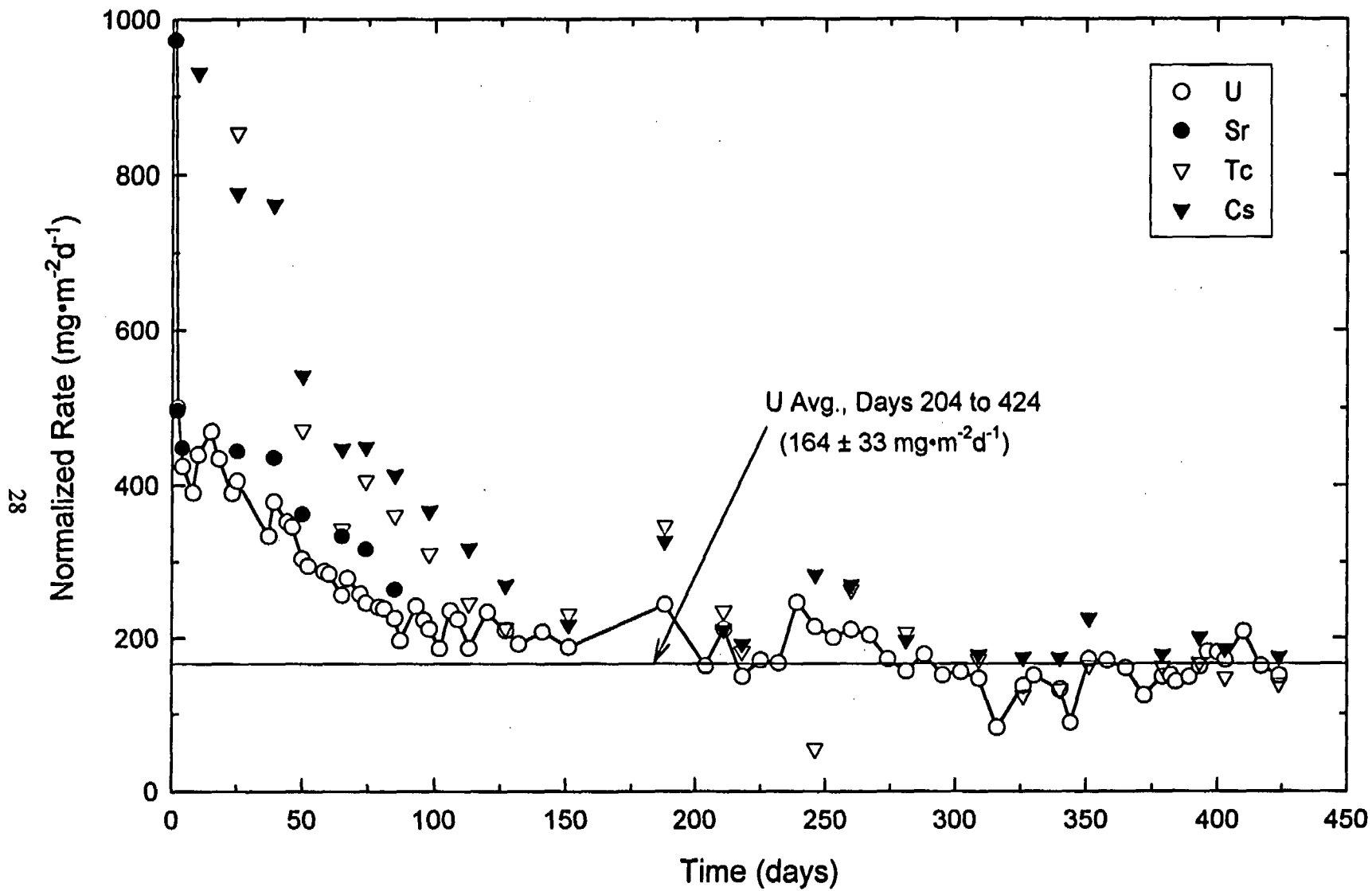


Figure 12. Dissolution Rate of Oxidized (U_4O_{9+x}) Particles of ATM-104 Spent Fuel in Aerated Water Containing $2 \times 10^{-2} \text{ M}$ Carbonate/Bicarbonate, $\text{pH} = 8$, at 25°C

Distribution

No. of Copies		No. of Copies	
	Offsite		
2	DOE/Office of Scientific and Technical Information T. Ahn Division of Waste Management U.S. Nuclear Regulatory Commission Washington, DC 20555 M. J. Apted QuantiSci 3900 South Wadsworth Blvd. Suite 555 Denver, CO 80235 R. Beyer Westinghouse Electric Corp. Bettis Atomic Power Laboratory PO Box 79 Westmislin, PA 15122-0079	6	Argonne National Laboratory 9700 S. Cass Ave. Argonne, IL 60439 Attn: J. L. Bates R. E. Einziger R. J. Finch P. Finn M. Goldberg J. C. Cunnane
14	Lawrence Livermore National Lab. University of California P.O. Box 808 Livermore, CA 94550 Attn: T. A. Busheck, L-206 C. K. Chou, L-638 W. L. Clarke, L-204 W. Halsey, L-204 L. Lewis, L-195 D. McCright, L-369 W. J. O'Connell, L-195 M. Revell, L-206 R. B. Stout (5), L-217 S. A. Steward, L-092	21	U.S. Department of Energy Yucca Mountain Site Characterization Project Office 101 Convention Center Drive P.O. Box 98608 Las Vegas, NV 89193-8608 Attn: R. W. Andrews/M&O J. A. Blink/LLNL P. R. Daniel/YMSCO N. Z. Elkins/LANL J. C. Farmer/LLNL R. Fish/M&O L. D. Foust/TRW D. C. Haught/YMSCO J. Lee/M&O B. Mann/M&O J. K. McCoy/M&O C. M. Newbury/YMSCO A. M. Simmons/YMSCO E. T. Smistad/YMSCO D. Stahl/M&O P. Stephens/REECO C. Stockman D. P. Stucker/YMSCO T. A. Thornton A. E. Van Luik/YMSCO T. M. Williamson/M&O

**No. of
Copies**

**No. of
Copies**

Foreign

4	AECL Research Whiteshell Laboratories Pinawa, Manitoba R0E 1L0 Canada Attn: L. Johnson D. Shoesmith S. Stroes-Gascoyne J. Tait J. Bruno QuantiSci Parc Tecnologic del Valles E-08290 Barcelona Spain		H. Matzke European Institute for Transuranic Elements Postfach 2340 D-76125 Karlsruhe Germany K. Ollilla VTT Chemical Technology Otakarri 3A PO Box 1404 FIN-02044 Espoo Finland
2	CIEMAT Avda. Complutense, 22 28040 Madrid Spain Attn: F. Mendez J. Serrano T. Eriksen Royal Institute of Technology Teknikringen 56 S-10044 Stockholm Sweden R. Forsyth Forsyth Consulting Stenbrinken 7 S-61134 Nykoping Sweden		J. Paul CEA-Valrho Marcoule DCC/DRDD/SCD B.P.171 F-30207 Bagnols-sur-Ceze France M. Skalberg Chalmers University of Technology Department of Nuclear Chemistry S-41296 Goteborg Sweden
		2	SKB PO Box 5864 S-10240 Stockholm SWEDEN Attn: K. Spahiu L. Werme
2	KFK/INE Postfach 3640 D-76021 Karlsruhe Federal Republic of Germany Attn: A. Loida B. Grambow	2	Studsvik Nuclear AB S-61182 Nykoping Sweden Attn: U. Eklund H. Christensen

**No. of
Copies**

- 2** **Universitat Politecnica Catalunya**
Dept. of Chemical Engineering
Avenida Diagonal 647, 4a Planta
E-08028 Barcelona
Spain
Attn: J. de Pablo
I. Casas

Onsite

DOE Richland Operations Office

R.G. Holt, S7-41

- 18** **Pacific Northwest Laboratory**

W. J. Gray (10), P7-27
J. M. Latkovick, K9-44
S. C. Marschman , P7-27
B. P. McGrail, K6-81
Technical Report Files (5)